INTERFERENCE ALIGNMENT (IA) AND COORDINATED MULTI-POINT (COMP) WITH IEEE802.11AC FEEDBACK COMPRESSION: TESTBED RESULTS

Per Zetterberg

Access Linnaeus Center
KTH Royal Institute of Technology, Osquldas väg 10,
SE-100 44 Stockholm, Sweden,
Email: perz@ee.kth.se

ABSTRACT

We have implemented interference alignment (IA) and joint transmission coordinated multipoint (CoMP) on a wireless testbed using the feedback compression scheme of the new 802.11ac standard. The performance as a function of the frequency domain granularity is assessed. Realistic throughput gains are obtained by probing each spatial modulation stream with ten different coding and modulation schemes. The gain of IA and CoMP over TDMA MIMO is found to be 26% and 71%, respectively under stationary conditions. In our dense indoor office deployment, the frequency domain granularity of the feedback can be reduced down to every 8th subcarrier (2.5MHz), without sacrificing performance.

Index Terms— interference alignment, coordinated multipoint, testbed, 802.11ac.

1. INTRODUCTION

Interference alignment (IA) is a theoretically promising scheme for dramatically increasing the spectrum efficiency of wireless systems, [1]. Prior work on experimentation with IA includes [2, 3, 4, 5, 6, 7] and [8]. The papers [2, 3, 4, 6] consider a scenario with three simultaneous MIMO 2×2 inks, while [8] consider 4×4 ([7] considers a 1×1 case utilizing a techique called blind IA which is not be considered in this paper). In the 2×2 case, IA should ideally provide three spatial streams while TDMA MIMO can only deliver two, which in principle should give a throughput gain of around 50% at high SNR. The paper [2] presents results from simulation on normalized versions of measured channels, and finds the degrees of freedom of IA and TDMA MIMO to agree with the theoretical predictions. The paper [3] presented the first over-the-air evaluation of IA with actual data transmission. The paper presents EVM measurements but bases channel capacity results on mutual information calculated from channel measurements. The paper finds that IA outperforms TDMA (17bits/s/Hz versus 11bits/s/Hz at the 40% level of the sum-rate CDF, see Figure 11 of [3]), but then no MIMO is applied in the TDMA case. The measurements were performed in a lecture room. The paper [8] investigates the degradation of IA due to channel estimation errors in the same testbed as [3], and finds them to be substantial. In the paper [6] we used an OFDM modulation which is close to the 802.11a/n/ac standards, and presented results from an indoor environment in both in LoS and NLoS locations (between rooms). The measurement scenario is clearly interference limited and shows fair agreement between theory and measurements, if dirty RF effects are catered for. The paper [8] considers an urban mixed outdoor-to-indoor and indoor-to-indoor scenario. The mobile-station is located indoors on the fifth floor of an urban building, two of the base-stations on roof-tops some 150 meters from the mobile, and the third base-station in the room adjacent to the mobile (there is only a single mobile-station, the other two are simulated). In the paper the performance of IA is analyzed by measuring the singular values of the interference at the receiver. Impressive 39dB interference suppression is achieved. However, only a single subcarrier is used - which should eliminate most nonlinear effects.

Prior CoMP experiments are found in [9, 10, 11] and [6]. The paper [9] presents experimental results from a real-time LTE implementation with two base-stations (BSs) and two mobile-stations (MSs), all using two antennas. The paper reports 4 to 22 times improvement compared to uncoordinated transmissions in the two cells. The paper [10] presents similar real-time implementations and reports 2.6 times gain over uncoordinated cells (see Table II of [10]). The paper [11], reports 31% and 55.3% gains over uncoordinated cells. In the paper [6] we argued that by modeling the error vector magnitudes (EVM) of the transmitter radios, fair agreement can be obtained between measured and real-world SINR ratios for CoMP.

Feedback compression in MIMO interference alignment has been studied in [12, 13, 14, 15] and many other papers.

In this paper, we extend the implementation of [6], with the use of the practical feedback compression defined in the IEEE802.11ac standard for single BS multi-user MIMO (MU MIMO), [16], and use it in the context of both IA and CoMP. The performance is assessed as a function of the frequency domain granularity of the feedback. We also introduce adaptive modulation and coding and thereby produce highly realistic performance results.

The paper is organized as follows. In Section 2 we give an overview of the implementation. The IEEE802.11ac single-cell MU-MIMO feedback scheme is reviewed in Section 4 where we also show how to apply it for IA and CoMP. In the section following, the air interface and the signal processing functions are described in more detail. The results are presented in Section 6. The paper is concluded in Section 7.

2. IMPLEMENTATION

In the considered scenario, there are three base- and mobile-stations each having two vertically polarized antennas. Under IA all three BSs simultaneously transmits a modulated stream to its associated

This work was done within the framework of the Swedish SSF sponsored RAMCOORAN project and the EU project RAMCOORAN. The HiATUS project acknowledges the financial support of the Future and Emerging Technologies program within FP7 for Research of the European Commission (FET Open grant number 265578).

978-1-4799-2893-4/14/$31.00 ©2014 IEEE

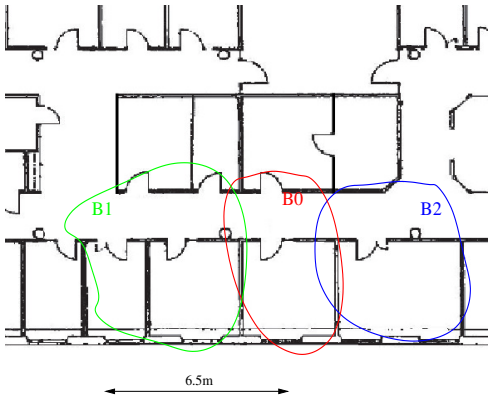

Fig. 1. Map over the measurement area

MS by means of linear precoding at the transmitter, and MMSE combining at the receiver.

As a baseline we use TDMA MIMO where each BS transmits two streams, but only one BS is active at a time. We also include two additional baselines. We call them full-reuse MIMO and full re-use SIMO. Full-reuse MIMO is identical to TDMA MIMO except all six streams are active all the time. If the interference between the BSs is small, this technique will be favorable. In full-reuse SIMO only one stream is transmitted from each BS, just as in IA. When only one of the two of interfering BSs is interfering (for instance the other one is blocked by a brick-wall), this technique will perform similar to IA since the receiver can reject the single remaining interferer.

In addition we include a technique which is superior to interference alignment, but more complex, namely joint transmission coordinated multipoint (CoMP). In this technique all the six transmitter antennas act as one BS with six distributed antennas. This technique requires all user data to be shared among the three BSs and phase coherence among the BS, which is not required in IA. Both IA and CoMP require precise time alignment and coordinated scheduling of transmissions between the BSs. The precise time alignment enables IA and CoMP to treat each subcarrier as an independent narrow-band system

In CoMP we use three streams (one per BS) just as in IA. Adding more streams could further increase the capacity of CoMP. This is a topic for future investigation. All the software is available at `sourceforge.net` under a GNU open source software license. The code can be found under the project names `fourmulti` and `iacomp`. The base-band processing of all BSs are done in one PC and the corresponding MSs processing in another. The individual nodes run as separate threads in the PCs. For a description of the hardware we refer the reader to [6].

The system has been calibrated so that the noise standard deviation is roughly the same in all receiver chains, $\sigma^2_{\text{nominal}}$. The value $\sigma^2_{\text{nominal}}$ is known by all nodes and is used in the receiver MMSE algorithm, in the feedback quantization, and the beamforming max-SINR algorithm.

The three BSs are placed near the ceiling in the positions indicated as B0, B1 and B2, in the map in Figure 1. The areas where the corresponding MS is located during the measurements are marked with red, green and blue color, respectively. The LoS measurements were made in the corridor while the NLoS measurements were made in the adjacent rooms.

D0	D1	D2	MCS 0–4, 2880 symbols or MCS 5–9, 1200 symbols

Fig. 2. Training block

3. AIR INTERFACE AND SIGNAL PROCESSING OVERVIEW

The air interface uses OFDM modulation with the same subcarrier spacing as 802.11a/n/ac namely 312.5kHz. Due to implementation constraints, we use only 38 subcarriers instead of the (at least) 58 used by 802.11n/ac. A cyclic prefix of 0.4μs is employed, which correspond to the short cyclic prefix of 802.11n/ac.

A coding and modulation gearbox with ten combinations of QAM modulations QPSK, 16QAM, 64QAM and 256QAM and LDPC codes with 1/2, 5/8 and 3/4 rate has been implemented. The performance of the gearbox is 2-5dB from the Shannon limit on AWGN channels in the 2 to 22dB SNR range.

When running the system, two frames are transmitted. The first frame contains six OFDM training symbols from the six transmitter antennas in the system. These pilots model the null data packet (NDP) of IEEE802.11ac, see [16]. The MSs estimates the channels based on these six OFDM symbols for all six transmitter antennas and all 38 subcarriers. These estimates are then compressed as described in Section 4. The result is then sent over wired Ethernet to the transmitter PC. In the BS PC, the channel state information is collected in the master thread, which calculates the beamforming weights according the max-SINR algorithm as described in Section 5. A second frame is then formatted and transmitted from all three BSs simultaneously 40ms after the training frame was transmitted (the measurements are done under stationary conditions). This frame is 3.2ms long and is divided into six identical subframes (for measurement purposes). Each subframe is divided into two so-called training blocks. A training block is formatted as indicated in Figure 2 above. The three symbols, D0, D1 and D2, are known pilot symbols pre-coded with the beamformer of stream 0,1 and 2, respectively. These symbols correspond to demodulation reference symbols in LTE nomenclature and correspond to the VHT-LTF field in 802.11ac. The MMSE receiver uses these three symbols to calculate the combiner weights i.e. a structured covariance matrix estimate is used. No frequency domain averaging of the channel estimates are done. Following these three training symbols are coding blocks which use MCS0 (MCS stands for coding and modulation scheme) to MSC4 in the first training block and MCS5 to MCS9 in the second. The reason for splitting the subframes into two training blocks, is the channel and sample-clock drifts that need to be compensated by the receiver. Tracking loops could maybe eliminate the need for the split. Before sending the combined samples to the detector, the effective noise variance is calculated by measuring the distance from the samples to the nearest constellation points. This noise variance estimate is used by the log-likelihood ratio (LLR) extractor. This re-estimation of the noise variance is done in order to account for the influence of distortions and residual interference.

4. FEEDBACK ACCORDING TO IEEE802.11AC

The feedback described in standard IEEE802.11ac seems to originate with [17] where it is called “simple feedback method for slowly time-varying channels”. In this scheme a singular value decomposition of the MIMO channel (for a certain subcarrier) is first performed

as $\mathbf{H} = \mathbf{USV}^H$. In single-user MIMO and single-cell multi-user MIMO, the $\mathbf{U}$ matrix, is of little use for the transmitter and therefore only the diagonal matrix $\mathbf{S}$ and the unitary matrix $\mathbf{V}$ need to be feed-back to the transmitter. When IA and CoMP are considered, several channel matrices are involved for each user. In this context the $\mathbf{U}$ matrix will be different for different links, and will be important to determine the interference subspaces at the receivers. To solve this problem, each MS will instead base its feed-back on the "big" $\mathbf{H}$ matrix, where the submatrices of the BSs have been concatenated. For instance the "big" $\mathbf{H}$ matrix of user k is given by

$$\mathbf{H}_k = [\mathbf{H}_{k,1}, \mathbf{H}_{k,2}, \mathbf{H}_{k,3}], \tag{1}$$

where $\mathbf{H}_{k,n}$ is the channel matrix between user k and BS n. The MS makes an SVD of this matrix as

$$\mathbf{H}_k = \mathbf{U}_k \mathbf{S}_k \mathbf{V}_k^H. \tag{2}$$

Since all signals received by the kth user will pass through $\mathbf{H}_k$, it is clear that $\mathbf{U}_k$ can be neglected. Thus, once the base-stations receive $\mathbf{U}_k$ and $\mathbf{S}_k$, they re-create the channel matrix as

$$\breve{\mathbf{H}}_k = \mathbf{S}_k \mathbf{V}_k^H, \tag{3}$$

from which the sub-matrices corresponding to different BSs can be extracted and applied in the max-SINR algorithm, see Section 5.

The 802.11ac feedback compression starts by phase rotating the columns of $\mathbf{V}$ so that the last row becomes real and positive. These phases do not need to be sent to the BS since demodulation reference signals are used to compensate for phase rotations of signal streams anyway. In the next step, the $\mathbf{V}$ matrix is multiplied by a diagonal matrix as

$$\tilde{\mathbf{V}} \leftarrow \text{diag}(\exp(j\phi_{1,1}), \ldots, \exp(j\phi_{m-1,1}), 1)\mathbf{V} \tag{4}$$

where the angles ϕ are chosen to remove the phases of the first column of $\mathbf{V}$. These angles ϕ are uniformly quantized with b_ϕ bits. Following this step, is a step where real-valued Givens rotations are applied to successively zero out the element (2,1) to (m,1) of $\tilde{\mathbf{V}}$ using angles $\psi_{2,1}, \ldots, \psi_{m,1}$. These ψ lie between 0 and $\pi/2$ and are quantized uniformly with b_ψ bits. The process continues in a similar familiar fashion for the remaining columns of $\mathbf{V}$. For the details we refer the reader to the Matlab/Octave functions available at `http://people.kth.se/~perz/packV/`, and to [17] and [16]. The total number of bits needed to feedback the $\mathbf{V}$ matrix is given by $((2m-1)n - n^2)(b_\phi + b_\psi)/2$.

In the IA case (with three BSs and MSs) we can actually reduce the number of bits by $2b_\phi$ by reducing the number of ϕ angles. This is done by dividing the $\mathbf{V}$ matrix in three parts as

$$\mathbf{V}^T = [\mathbf{V}_0^T, \mathbf{V}_1^T, \mathbf{V}_2^T]. \tag{5}$$

Since the signals transmitted from BS0, BS1 and BS2 only propagates through $\mathbf{V}_0$, $\mathbf{V}_1$ and $\mathbf{V}_2$, respectively, the beamforming effect is not changed if these blocks are rotated by a complex phasor. Thus we modify $\mathbf{V}_0$ and $\mathbf{V}_1$ so that their upper-left element becomes positive and real-valued. This will make the corresponding ϕ values zero by definition and don't need to be feed back to the transmitter. In the implementations presented in the paper, this reduction of the number of feedback bits for IA has been implemented.

Since OFDM is used, there is one $\mathbf{H}$ matrix per subcarrier. In the 802.11ac standard there is a parameter N_g which determines the frequency domain granularity of the feedback. If $N_g = 1$ then the feedback of $\mathbf{V}$ is done on every subcarrier, if $N_g = 2$ the feedback is done on roughly every other subcarrier and so on. The settings $N_g = 1, 2, 4$ are defined in the standard. We have augmented this with $8, 16, 38$ since this seems to be an effective way of reducing the number of feedback bits. The number of bits for the angles b_ϕ and b_ψ (see above), can have the values $b_\psi = 5$ and $b_\phi = 7$ or $b_\psi = 7$ and $b_\phi = 9$ according to the standard. Herein, only the latter values has been used.

The signal to noise ratio (SNR) is reported with half the granularity of the $\mathbf{V}$ matrix i.e., the SNR is only reported for half of the subcarriers on which the $\mathbf{V}$ matrix is reported. The SNR is reported as corresponding to the diagonal elements of the matrix $\mathbf{S}$ (called streams in 802.11ac). In our case we have divided the elements with noise standard deviation σ_{nominal} mentioned in Section 2. The reporting is done in two steps. First the SNR averaged (in dB) over the whole band (per singular value) is reported. We interpret this as the average over the subcarriers for which the SNR is reported. This average is then uniformly quantized with eight bits in the range from -10dB to 53.75dB. Having obtained the average SNR per stream, the SNR per reported subcarrier is given as the difference (the delta) between the subcarrier SNR and its average (in dB). The delta is reported as an integer between -8dB and +7dB, thus requiring four bits.

In the BS, we first reconstruct the SNR per reported subcarrier. We then employ linear interpolation (in dB) to obtain the SNR for all the subcarriers where $\mathbf{V}$ is feed back. With these two entities at hand, the channel matrices are reconstructed as in (3). The beamforming weights are calculated as described in Section 5 based on these channel matrices. On subcarriers where there is no feedback available, the beamformer of the nearest reported subcarrier is used. Thus no interpolation is attempted.

5. BEAMFORMER IMPLEMENTATION

We use the max-SINR algorithm of [18] to iteratively maximize the SINR with respect to the receiver- and transmitter-filters in both the IA and CoMP case. Compared to the max-SINR implementation in [6] two improvements have been made. First, we initialize the transmitter filters in the closed form solution in Appendix II of [1] for IA. For CoMP we initialize the transmitter filters in the pseudo-inverse of the eigenbeamformers. Secondly, we have added a regularization term to the noise as

$$\sigma_k^2 = \sigma_{\text{nominal}}^2 + \mu \sum_j \|\mathbf{H}_{k,j}\|^2, \tag{6}$$

with $\mu = 0.001$ to help robustify the system. Equation is based on the assumption that hardware impairments add a noise proportional to the total received power.

6. RESULTS

The system was run during night-time with no people moving in the environment. In total 22 LoS and 21 NLoS positions were selected for each of the three MSs. There were several wavelengths between these positions. For all these positions IA and CoMP and all the reference schemes were run in a sequence with an interval of 0.34 seconds between the schemes. For each run we get six throughput values by finding the highest MCS with no bit errors, see Section 3. Six seconds later, all the schemes was run again in the same position with a different value of N_g, see Section 4. Finally, we also test the performance without quantization but with frequency domain granularity. The reference schemes were repeated for each value of N_g, to "calibrate" the throughput gains against the possible influence of

channel fluctuations. The average signal to interference ratio (disregarding beamforming) is 3.2dB. The signal to noise ratio (averaged over antennas and subcarriers) varies between 35 and 60dB in the measurements - thus the system is truly interference limited.

Figure 3 and 4 shows the results from LoS and NLoS, respectively. We note that the results in LoS and NLoS are similar for CoMP, and TDMA-MIMO while the results for IA, full-reuse SIMO and full-reuse MIMO, have improved by 25%, 77% and 76%, when going from LoS to NLoS respectively. The reason for this difference can be seen in Figure 5. In Figure 5 each 'x' represents one mobile LoS position. Since there are two interfering BSs, we can define two C/I for each point. The x-axis of each point represents the lower of the two C/I and the y-axis the higher. Thus by construction each 'x' is located above the blue dashed $y = x$ line. The red 'o' points indicates the corresponding statistic for the NLoS points. From Figure 5 we see that the C/I is higher in NLoS than in LoS. Moreover, in LoS it common that one of the interfering BS is much stronger than the other. This is probably due to the influence of the walls. The schemes IA, full-reuse SIMO and full-reuse MIMO, benefit from the higher C/I. Full-reuse SIMO further benefit when only one interfering BS is strong, since it is able to reject one interferer using its two receive antennas.

From the results we conclude that there is no loss of performance due to the quantization. In LoS only the lowest frequency domain granularity implemented, $N_g = 38$ results in a loss significant loss while $N_g = 16$ incurs a minor loss. In NLoS a loss of 8% and 3% occurs at $Ng = 8$ for IA and CoMP, respectively. For $Ng = 16$ the loss increases to 15% for both schemes. . By averaging all measurements where $N_g < 16$, we obtain the following throughputs averaged over LoS and NLoS (in sum throughput bits/symbol/subcarrier) IA:11.1 , CoMP:15.1, TDMA-MIMO:8.8, full-reuse SIMO:6.4 , full-reuse MIMO:2.2.

In Figure 6 we present simulation results obtained for IA using the exact same C++ code as was running in our real system, but using propagation models with various levels of RMS delay-spread, representative for indoor WLAN, [19]. We first notice that the maximum throughputs are higher than in the real system. This is because the real system is suffering from distortions, see [6]. The simulated performance degrades quickly when N_g is increased. It is possible that some of this effect is masked by the distortions in the real system. However, the simulation results show that $N_g <= 4$ is necessary for typical conventional deployments. However, our measurements shows that N_g values greater than four would be useful for very dense deployments. Identical simulations for CoMP showed less sensitivity to N_g.

7. CONCLUSION

We have implemented 802.11ac based feedback compression in a real system employing three BS and three MS. The throughput has been assessed by probing the spatial channels with a sequence of coding and modulation schemes. The gain of IA and CoMP over TDMA MIMO is 30% and 70% , respectively under stationary conditions. In our dense deployment, the frequency domain granularity of the feedback can be reduced down to about every 8th subcarrier (5MHz), without sacrificing performance. The feedback compression of 802.11ac does not incur any performance loss.

In order to estimate the overhead loss of IA and CoMP under non-stationary conditions, the required update rate need to be known. This will be a topic for future work.

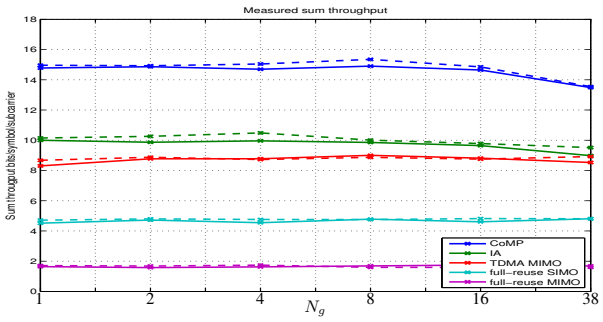

Fig. 3. Measured sum throughput in LoS scenarios. The dotted line are the results without compression

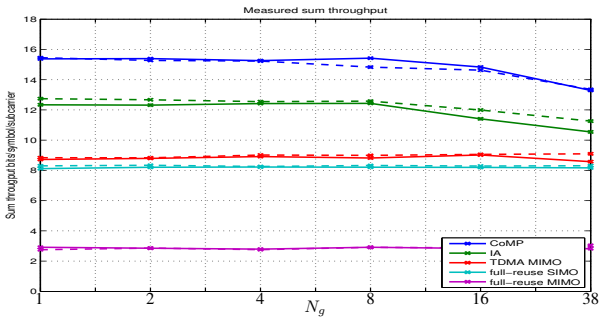

Fig. 4. Measured sum throughput in NLoS scenarios. The dotted line are the results without compression

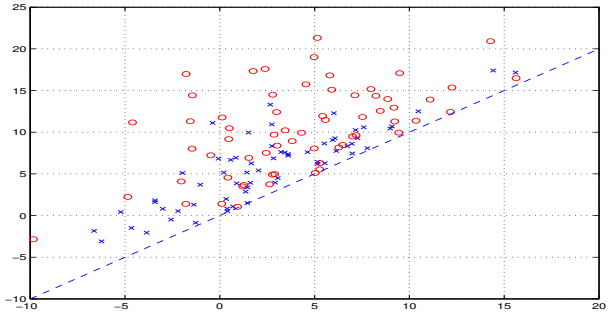

Fig. 5. The C/Imin versus C/Imax. 'X': LoS, 'o':NLoS

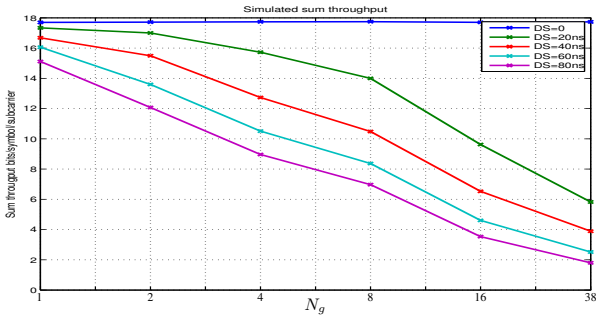

Fig. 6. Simulated sum throughput for IA as a function of N_g

8. REFERENCES

[1] V.R. Cadambe and S.A. Jafar, "Interference alignment and degrees of freedom of the K -user interference channel," *IEEE Transactions on Information Theory*, vol. 54, no. 8, pp. 3425 –3441, aug. 2008.

[2] O. El Ayach, S.W Peters, and R.W Heath, "The feasibility of interference alignment over measured MIMO-OFDM channels," *IEEE Transactions on Vehicular Technology*, vol. 59, no. 9, pp. 4309 –4321, nov. 2010.

[3] Ó. González, D. Ramírez, I. Santamaria, J.A. García-Naya, and L. Castedo, "Experimental validation of interference alignment techniques using a multiuser MIMO testbed," in *Smart Antennas (WSA), 2011 International ITG Workshop on*, feb. 2011.

[4] J.A. García-Naya, L. Castedo, Ó. González, D. Ramírez, and I. Santamaria, "Experimental evaluation of interference alignment under imperfect channel state information," in *European Signal Processing Conference (EUSIPCO 2011)*, Barcelona, Spain, aug. 2011.

[5] R. Brandt, H. Asplund, and M. Bengtsson, "Interference alignment in frequency - a measurement based performance analysis," in *Systems, Signals and Image Processing (IWSSIP), 2012 19th International Conference on*, 2012, pp. 227–230.

[6] P. Zetterberg and N. Moghadam, "An experimental investigation of SIMO, MIMO, interference-alignment (IA) and coordinated multi-point (CoMP)," in *International Conference on Systems, Signals and Image Processing (IWSSIP)*, April 2012.

[7] K. Miller, A. Sanne, K. Srinivasan, and S. Vishwanath, "Enabling real-time interference alignment: Promises and challenges," in *ACM International Symposium on Mobile Ad Hoc Networking and Computing (MobiHoc)*, 2012.

[8] M. Mayer, G. Artner, G. Hannak, M. Lerch, and M. Guillaud, "Measurement based evaluation of interference alignment on the vienna MIMO testbed," in *The Tenth International Symposium on Wireless Communication Systems*, August 2013.

[9] V. Jungnickel, A. Forck, S. Jaeckel, F. Bauermeister S. Schubert, S. Wahls S, L. Thiele, H. Droste, and G. Kadel, "Field trials using coordinated multi-point transmission in the downlink," in *3rd International Workshop on Wireless Distributed Networks (WDN), held in conjunction with IEEE PIMRC 2010*. September 2010, IEEE.

[10] D. Li, Y. Liu, H. Chen, Y Wan, Y Wang, C Gong, and L. Cai, "Field trials of downlink multi-cell MIMO," in *Wireless Communications and Networking Conference (WCNC), 2011 IEEE*, march 2011, pp. 1438 –1442.

[11] J. Holfeld, I Riedel, and G Fettweis, "A CoMP downlink transmission system verified by cellular field trials," in *European Signal Processing Conference (EUSIPCO)*, aug. 2011.

[12] R. T. Krishnamachari and M. K. Varanasi, "Interference alignment under limited feedback for MIMO interference channels," in *Internation Symposium on Information Theory*, Austin, Texas, USA, 2010.

[13] J.S. Kim, S.H. Moon, S.R. Lee, and I. Lee, "A new channel quantization strategy for MIMO interference alignment with limited feedback," *Wireless Communications, IEEE Transactions on*, vol. 11, no. 1, pp. 358–366, June 2012.

[14] H. Farhadi, C. Wang, and M. Skoglund, "On the throughput of wireless interference networks with limited feedback," in *Information Theory Proceedings (ISIT), 2011 IEEE International Symposium on*, Saint-Petersburg, Russia, August 2011, pp. 762–766.

[15] M. Rezaee and M. Guillaud, "Limited feedback for interference alignment in the k-user MIMO interference channel," in *IEEE Information Theory Workshop (ITW)*, 2012, pp. 667–671.

[16] R. Porat, E. Ojard, N. Jindal, M. Fischer, and V. Erceg, "Improved MU-MIMO performance for future 802.11 systems using differential feedback," in *UCSD Information Theory and Applications Workshop*, Catamaran Resort, San Diego, USA, 2013, pp. 1–5.

[17] J.C Roh and B.D Rao, "Efficient feedback methods for MIMO channels based on parameterization," *IEEE Transactions on Wireless Communications*, vol. 6, no. 1, pp. 282–292, 2007.

[18] K. Gomadam, V.R. Cadambe, and S.A. Jafar, "Approaching the capacity of wireless networks through distributed interference alignment," in *IEEE Global Telecommunications Conference, 2008 (GLOBECOM 2008)*, 30 2008-dec. 4 2008, pp. 1 –6.

[19] V. Erceg et. al, "TGn channel models," Tech. Rep. IEEE 802.11-03/940r, IEEE, Jan 2004.